Solid State Communications 182 (2014) 10–13

Contents lists available at ScienceDirect

Solid State Communications

journal homepage: www.elsevier.com/locate/ssc

Magnetization characteristic of ferromagnetic thin strip by measuring anisotropic magnetoresistance and ferromagnetic resonance

Ziqian Wang *, Guolin Yu, Xinzhi Liu, Bo Zhang, Xiaoshuang Chen, Wei Lu

National Laboratory for Infrared Physics, Shanghai Institute of Technical Physics, Chinese Academy of Sciences, 500 Yutian Road, Shanghai 200083, China

ARTICLE INFO

Article history:
Received 18 September 2013
Received in revised form
25 November 2013
Accepted 28 November 2013
by X.C. Shen
Available online 7 December 2013

Keywords:
A. Permalloy thin strips
D. Anisotropic magnetoresistance
D. Demagnetization
D. Magnetic anisotropy

ABSTRACT

The magnetization characteristic in a Permalloy thin strip is investigated by electrically measuring the anisotropic magnetoresistance and ferromagnetic resonance in in-plane and out-of-plane configurations. Our results indicate that the magnetization vector can rotate in the film plane as well as out of the film plane by changing the intensity of external magnetic field of certain direction. The magnetization characteristic can be explained by considering demagnetization and magnetic anisotropy. Our method can be used to obtain the demagnetization factor, saturated magnetic moment and the magnetic anisotropy.

1. Introduction

Anisotropic magnetoresistance (AMR) effect, which is resulted from the anisotropy of spin–orbit interaction in ferromagnetic materials [1,2], was first discovered by Thomson in 1857 [3]. This effect bears an essential role for both scientific perspectives and technological applications [4–8]. AMR is manifested in the dependence of the resistivity on the angle between current and magnetization direction [1,2], and is given by

$$R = R_0 + R_A - R_A \sin^2\theta. \quad (1)$$

Here R_0 represents the resistance while the magnetization **M** is perpendicular to the induced current, R_A is the decrement resistance, and θ is the angle of magnetization **M** with respect to radio-frequency (*rf*) current which is induced by microwave. In ferromagnetic devices of certain structures, **M** is parallel to the effective magnetic field $\mathbf{H}_{eff}$, including external field $\mathbf{H}_{ex}$, anisotropy built-in field $\mathbf{H}_a$ and demagnetization field $\mathbf{H}_d$.

The purpose of our work is to obtain magnetization characteristic of a ferromagnetic thin strip through AMR measurement. Ferromagnetic resonance (FMR) detection is considered as an ancillary method to determine the magnetization based on fitting the measured FMR dispersion curves via Kittel's theory [9].

2. Material and methods

The present work is performed on a Permalloy ($Ni_{80}Fe_{20}$, Py) thin film deposited on a $5 \times 6\ mm^2$ Gallium Arsenide (GaAs) single crystal substrate. This polycrystalline structured Py film is patterned to a stripe shape by photolithography and lift off techniques: a GaAs single crystal substrate is covered positive photoresist. In the following a negative image mask of the intended stripe structure is used to expose the photoresist. Afterwards the substrate is mounted in a high vacuum deposition chamber in which Py is molten to generate a ballistic flux of Nickel–Iron clusters that slowly covers the sample with a typically 50 nm thick Py layer. During the lift-off process, the Py film is subjected to ultrasonic and heating. The remaining structure is a Permalloy stripe with Permalloy leads and contacts. The dimensions of our sample are: length = 2400 μm, width = 200 μm and thickness = 50 nm.

The Py strip is fixed on a rotatable holder by an adjustable wedge. The external magnetic field, represented as $\vec{H}_{ex} = (H_x, H_y, H_z)$, encloses an intersection angle α with the long-axis of the strip, and β represents the dip of the wedge. Accurate α and β are recorded by a readout on the holder and a goniometer. AMR is measured by detecting the resistance between two electrodes at each side of the strip's length, as illustrated in Fig. 1(a). In FMR measurement, modulated microwave is propagating to the holder normally through a rectangular waveguide of X band, while the modulation frequency is 5.37 kHz. The FMR signals are also electrically measured in field-swept mode by using a lock-in amplifier connecting those two electrodes via gold bonding wires and coaxial cables.

* Corresponding author. Tel.: +86 18805101962.
E-mail addresses: ziqian86@mail.sitp.ac.cn (Z. Wang), yug@mail.sitp.ac.cn (G. Yu), bozhang@mail.sitp.ac.cn (B. Zhang), xschen@mail.sitp.ac.cn (X. Chen), luwei@mail.sitp.ac.cn (W. Lu).

0038-1098/$ - see front matter © 2013 Elsevier Ltd. All rights reserved.
http://dx.doi.org/10.1016/j.ssc.2013.11.034

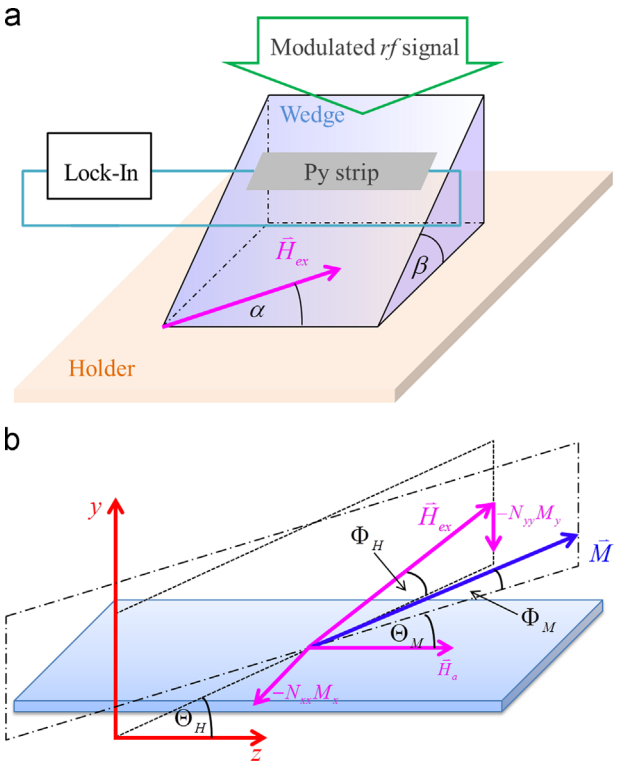

Fig. 1. (Color online) (a) The schematic of our experiment and (b) the coordinate system used in this article. The *rf* signal and lock-in amplifier are only applied in FMR measurement. The demagnetization field along x and y direction are also notified as $-N_{xx}M_x$ and $-N_{yy}M_y$.

The coordinate system we select in this article is demonstrated in Fig. 1(b). The long axis of the thin strip is set as z-axis, the direction perpendicular to the strip's plane is defined as y-axis, and the strip lies in the xz-plane. Φ_H, Φ_M are recorded as the misalignments of $\mathbf{H}_{ex}$ and $\mathbf{M}$ with respect to xz-plane. The in-plane components of $\mathbf{H}_{ex}$ and $\mathbf{M}$ enclose the angles Θ_H, Θ_M with z-axis, respectively. Hence Θ_H, Φ_H, α and β follows the relations as $\Theta_H = \tan^{-1}(\tan\alpha\cos\beta)$ and $\Phi_H = \sin^{-1}(\sin\alpha\sin\beta)$.

In Section 3.1, AMR and FMR measurements in weak $\mathbf{H}_{ex}$ are illustrated, and both of $\mathbf{H}_a$ and $\mathbf{H}_d$ are taken into account. We will show how $\mathbf{M}$ rotates from parallel to $\mathbf{H}_a$ via changing the magnitude of $\mathbf{H}_{ex}$ generated by an electromagnet at room temperature. The detailed process of obtaining the demagnetization factors and magnetization through AMR and FMR experiments is also introduced in this section. For further investigating, AMR in out-of-plane configuration in stronger $\mathbf{H}_{ex}$ is discussed in Section 3.2. In this section, the Py thin strip is placed in $\mathbf{H}_{ex}$ produced by a cryomagnet, which is carried out at liquid helium temperature.

3. Results and discussion

3.1. Weak external field condition

It is noted as "weak field condition" when the magnitude of $\mathbf{H}_{ex}$ is smaller than 2000 Oe. The measured AMR and FMR data of this Py thin strip in in-plane and out-of-plane configurations are shown in Fig. 2. Meanwhile, the demagnetization coefficient and $\mathbf{M}$ are obtained via fitting these experimental results by selecting appropriate models. Fig. 2(a) shows the measured sheet resistance R versus $\mathbf{H}_{ex}$ at different Θ_H in in-plane magnetized configuration. It is illustrated that R reaches its maximum at $\mathbf{H}_{ex}=0$, hence $\mathbf{M}$ is parallel, or anti-parallel, to z-axis as a higher resistance state without external magnetic field. The increment of R achieved by decreasing the magnitude of $\mathbf{H}_{ex}$ implies $\mathbf{M}$'s rotation from parallel with $\mathbf{H}_{ex}$ to z-axis, as demonstrated in Eq. (1). The direction of $\mathbf{M}$ at zero-field state is caused by $\mathbf{H}_a$, the anisotropic built-in field. $\mathbf{H}_a$ is along with z-axis because of the lowest free energy for thin strip structure in this direction.

Here we assume $\mathbf{H}_a$ as a static filed, which is parallel to z-axis and is expressed as $\vec{H}_a = (0,\ 0,\ H_a)$. The effect of other important factors on the rotation of $\mathbf{M}$ is the demagnetization field $\mathbf{H}_d$, which depends on $\mathbf{M}$. The relationship between $\mathbf{H}_d$ and $\mathbf{M}$ is written by $\vec{H}_d = -(N_{xx}M_x,\ N_{yy}M_y,\ N_{zz}M_z)$, where N_{xx}, N_{yy} and N_{zz} are the demagnetization factors in x, y and z directions, respectively. The demagnetization factors satisfy the correlation of $N_{xx}+N_{yy}+N_{zz}=1$ for *SI* and $N_{xx}+N_{yy}+N_{zz}=4\pi$ for *CGS* [11]. Accordingly, the yielded relations between $\mathbf{M}$ and $\mathbf{H}_{ex}$ are

$$\frac{H_x - N_{xx}M_x}{M_x} = \frac{H_y - N_{yy}M_y}{M_y} = \frac{H_z + H_a}{M_z},$$

$$H_x = |\vec{H}_{ex}|\cos\Phi_H\sin\Theta_H, H_x = |\vec{H}_{ex}|\sin\Phi_H,$$

$$H_z = |\vec{H}_{ex}|\cos\Phi_H\cos\Theta_H,$$

$$M_x = |\vec{M}|\cos\Phi_M\sin\Theta_M, M_y = |\vec{M}|\sin\Phi_M,$$

$$M_z = |\vec{M}|\cos\Phi_M\cos\Theta_M \tag{2}$$

The demagnetization field along z-axis is neglected since N_{zz} is much smaller than N_{xx} and N_{yy} in thin strip structure, as shown in Fig. 1(b). It is difficult to provide analytical solutions for Eq. (2), however getting numerical solutions is not a hard task. We use the numerical method to fit the experimental data. In in-plane configuration under weak field condition, $\Phi_H=\Phi_M=0$ and $H_y=0$, consequently Eq. (2) can be transformed as

$$\frac{|\vec{H}_{ex}|\sin\Theta_H - N_{xx}|\vec{M}|\sin\Theta_M}{|\vec{M}|\sin\Theta_M} = \frac{|\vec{H}_{ex}|\cos\Theta_H + H_a}{|\vec{M}|\cos\Theta_M}. \tag{3}$$

Considering $\Phi_H=\Phi_M=0$, we have $\theta=\Theta_H$. Taking the numerical results of Eq. (3) into Eq. (1), $\mathbf{H}_a$ and $N_{xx}M_x$ are obtained. R_0 and R_A can be recorded directly through Fig. 1 as $R_0=87.7\ \Omega$ and $R_a=1.5\ \Omega$. Other fitted results are $H_a=1.95$ Oe and $N_{xx}M_x=5.1$ Oe.

The demagnetization factor N_{yy} is significantly larger than N_{xx} according to the thin strip structure. If $\mathbf{H}_{ex}$ consists of y-component, $\mathbf{M}$ should be misaligned away to $\mathbf{H}_{ex}$, which causes the surface magnetic charges in each side of xz-plane [10]. These surface magnetic charges generate a demagnetization field inside the sample with its direction opposite to the y-component of $\mathbf{H}_{ex}$, and finally prohibit the misalignment of $\mathbf{M}$. According to the shape of our sample, the demagnetization field generated by a very slight y-component of $\mathbf{M}$ can offset the y-component of $\mathbf{H}_{ex}$. Thus, only the xz-component of $\mathbf{H}_{ex}$ is worth to be considered, the motion of $\mathbf{M}$ according to changing $\mathbf{H}_{ex}$ is almost in-plane, and we have

$$\frac{|\vec{H}_{ex}|\cos\Phi_H\sin\Theta_H - N_{xx}|\vec{M}|\sin\Theta_M}{|\vec{M}|\sin\Theta_M} = \frac{|\vec{H}_{ex}|\cos\Phi_H\cos\Theta_H + H_a}{|\vec{M}|\cos\Theta_M}, \tag{4}$$

$\Theta_M \approx \theta$.

The larger out-of-plane component of $\mathbf{H}_{ex}$ can be provided by increasing the dip angle β of the wedge. Comparating to the in-plane $\mathbf{H}_{ex}$, larger out-of-plane $\mathbf{H}_{ex}$ is needed for obtaining the same $\mathbf{H}_{eff}$ and θ, as showing in Fig. 2(b).

The calculated magnitudes of $\mathbf{M}$ is obtained by fitting FMR experiment. The dispersion curves in different configurations are recorded in Fig. 2(c). For an in-plane $\mathbf{M}$ assisted with microwave in a magnetic field $\mathbf{H}$, the resonant frequency f_r for the *rf* signal is given by $2\pi f_r = \gamma\sqrt{[H+(N_{yy}-N_{zz})M][H+(N_{xx}-N_{zz})M]}$ [9]. In our sample, we have $H = H_{eff} = |\vec{H}_{ex}+\vec{H}_d+\vec{H}_a|$ and $\gamma = 181\mu_0\ \mathrm{GHz/T}$ for Py, here μ_0 is the permeability of vacuum. The magnitude of $\mathbf{H}_{ex}$